A geological model of the buried Tiber River valley beneath the historical centre of Rome

Un modèle géologique du remplissage alluvial de la vallée du Tibre sous le centre historique de Rome

F. Bozzano · A. Andreucci · M. Gaeta · R. Salucci

Abstract The study develops a geological/geotechnical model of the filling of the buried Tiber River valley in the area of Rome. The approach has been multidisciplinary: the fill sediments have been analysed in detail and are given on a cross section based on either the observations of 57 borehole cores and/or the laboratory tests on various types of samples. Information regarding the geology, geomorphology, climate, hydrographic network, urban development and history of the Rome area has been used to interpret this section and to extrapolate the data to the historical centre of Rome in order to formulate the model. The proposed model is a global forecasting rather than a detailed one and can be used as a starting point for projects to be conducted in the Tiber River alluvium or for defining a specific approach to technical problems linked to these projects.

Résumé L'objectif de l'étude présentée est d'établir un modèle géologique-géotechnique du remplissage de la plaine alluviale du Tibre dans la région de Rome. L'approche est multidisciplinaire. Les sédiments de remplissage ont été finement analysés sur une coupe basée soit sur les observations de carottes de 57 sondages, ou sur des essais de laboratoire sur divers types d'échantillons. Des données relatives à la géologique, la géomorphologie, le climat, le réseua hydrographique, le développement urbain et l'histoire de la région de Rome ont été utilisées pour interpréter cette coupe et pour extrapoler les données au centre historique de Rome, dans le but d'établir un modèle. Le modèle proposé est un modéle global prédictif, différent d'un modèle détaillé, qui peut être utilisé comme un point de départ pour des projets qui seront développés dans le corps alluvial de la plaine du Tibre, ou pour définir une approche spécifique de problèmes techniques en rapport avec ces projets.

Key words Tiber River valley · Lithotypes · Geometrical relationships · Physical characteristics · Geomechanical parameters · Geological and geotechnical model

Mots clés Vallée du Tibre · Lithotypes · Relations géométriques · Caractéristiques physiques · Paramètres géomécaniques · Modèle géologique et géotechnique

Received: 26 July 1999 · Accepted: 25 October 1999

F. Bozzano (✉) · A. Andreucci · M. Gaeta · R. Salucci
Università degli Studi di Roma La Sapienza, Dipartimento di Scienze della Terra, Piazzale Aldo Moro 5, 00185 Roma, Italy
e-mail: francesca@geoappli1.geo.uniroma1.it
Fax: +39-6-4454729

Introduction

The city of Rome, with its approximately 2.8 million inhabitants, is located about 25 km from the Tyrrhenian Sea. Built upon the banks of the Tiber River (Figs. 1 and 2), the city represents one of the many examples of a metropolis built on the alluvial plain of an important river. The first evidence of settlements in the Rome area goes back to the fourteenth century B.C., while the true birth of the city occurred during the eighth century B.C. During its more than 2000-year history, Rome has undergone various phases of expansion, stability and reduction (Staderini 1998); since 1950 the city has extended over an area of more than 300 km^2. In addition to the numerous histori-

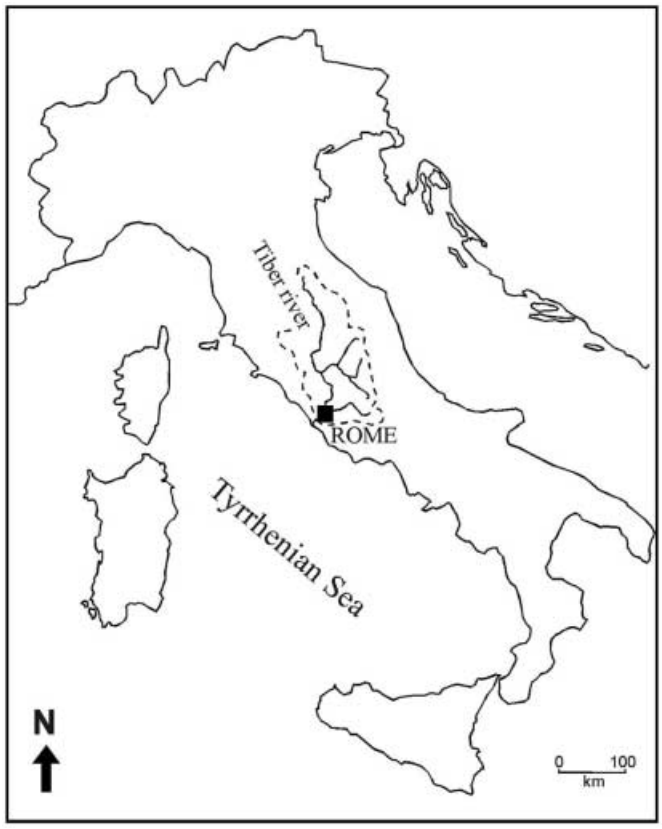

Fig. 1
The Tiber River basin

cally significant works of art and architecture created during its long and colourful history, Rome has also developed a complex urban fabric which will require proper management and conservation if the city is to facilitate this growth into the 21st century. This will include improving the urban transport system through the construction of new subway lines and modification of the road network as well as defining proper criteria for the choice and creation of new urban areas. In addition, it will be necessary to safeguard existing buildings from the potential collapse of subterranean cavities (Crescenzi et al. 1995; Lanzini 1995; Federici and Santoro 1997), slope movement along hill slopes (Fossa Mancini 1922; Amanti et al. 1995; Bozzano et al. 1998), differential settlement of foundation sediments (Calabresi et al. 1980; Amanti et al. 1995) or the local amplification of seismic waves (Fah et al. 1993; Boschi et al. 1995; Moczo et al. 1995; Donati et al. 1999). These examples clearly demonstrate the relationship that exists between the urban structure and the geological units on which it is built.

To date, knowledge of the geology of the Rome area has been based on a number of successive studies, beginning with the first geological maps of the city (e.g. Tellini 1893) and continuing with the publication of the monograph *La Geologia della Città di Roma* (Ventriglia 1971) and the compilation *La Geologia di Roma: Il Centro Storico* (Funiciello 1995) on which the geological map and profile given in Figs. 3 and 4, respectively, were based. The figures emphasise the presence of the large, recent alluvial bodies of the Tiber River and its tributaries within the older formations. The lithological setting and geotechnical characteristics of these alluvial deposits are poorly defined, however, due to the lack of outcrops and the intrinsic heterogeneity and heterotopy of the sediments. For this reason only limited data of this type are available from stratigraphic logs and ground investigation cores. Nevertheless, it is important to note that around 35% of the historical centre of Rome is built on the alluvial plain of the Tiber River or its tributaries (Fig. 3) and that several new structures are being built, or will soon be built, on or within these deposits. This is particularly important as it has been shown that the seismic impedance ratio between these alluvial deposits and the host formations is responsible for a greater concentration of earthquake damage within this urban area of the Tiber River alluvial plain (Ambrosini et al. 1986; Cifelli et al. 1997).

From this background, the objective of the present study was to develop a geological/geotechnical model of the buried Tiber River valley in the area of Rome. The approach adopted has been multidisciplinary, such that data regarding the geology, geomorphology, climate, hydrographic network, urban development and history of the Rome area have been used to interpret (and extrapolate) the cross section constructed through the alluvial body based on the study of the lithology, composition and geotechnical properties of core samples from 57 boreholes.

Geological setting

The city of Rome has developed in an area of the lower Tiber River valley between the Alban Hills Volcanic District (AHVD) to the south east and the Sabatini Mountains Volcanic District (SMVD) to the north west (Fig. 5). The oldest sediments outcropping in the city are represented by the "Monte Vaticano Unit", which is characterised by Middle-Upper Pliocene grey-blue clays (Marra and Rosa 1995a; Carboni and Iorio 1997) with decimetre-scale intercalations of sands. This formation generally dips between 4 and 20° towards the north west. It outcrops predominantly in the right bank of the Tiber River, at the base of the hills of Monte Mario, Vaticano and Gianicolo (Fig. 3) and represents the continuous bedrock of the Rome area (Fig. 4).

Overlying this substratum are the Lower Pleistocene "Monte Mario", "Monte Ciocci" and "Monte delle Piche" Units. The first and last units are marine sediments, whereas the middle is a 10- to 20-m-thick epicontinental deposit of gravels and sands (Marra 1993) whose stratigraphical unit is still being debated in the literature (Ambrosetti and Bonadonna, 1967; Bellotti et al. 1994). The 60-m-thick Monte Mario Unit is transgressive on the Monte Vaticano Unit (Marra and Rosa 1995a; Milli 1997) and outcrops on the hills of Monte Mario, Vaticano and Giani-

Fig. 2
Aerial photograph of historical centre of Rome. Approx. scale 1:20,000. (Courtesy of Società Aereofotografica e Rilevamenti Aerofotogrammetrici, Nistri)

colo in direct contact with the Pliocene bedrock. It is characterised by a lower, predominantly clayey-silty portion which passes upwards through grey sands, yellow marine sands with frequent "panchina" levels (skeletal sandstones) and finally a lagoon clay deposit. In contrast, the Monte delle Piche Unit which outcrops to the south west of the city outside the area shown in Fig. 3 varies from a basal clay succession to an upper clayey sand.

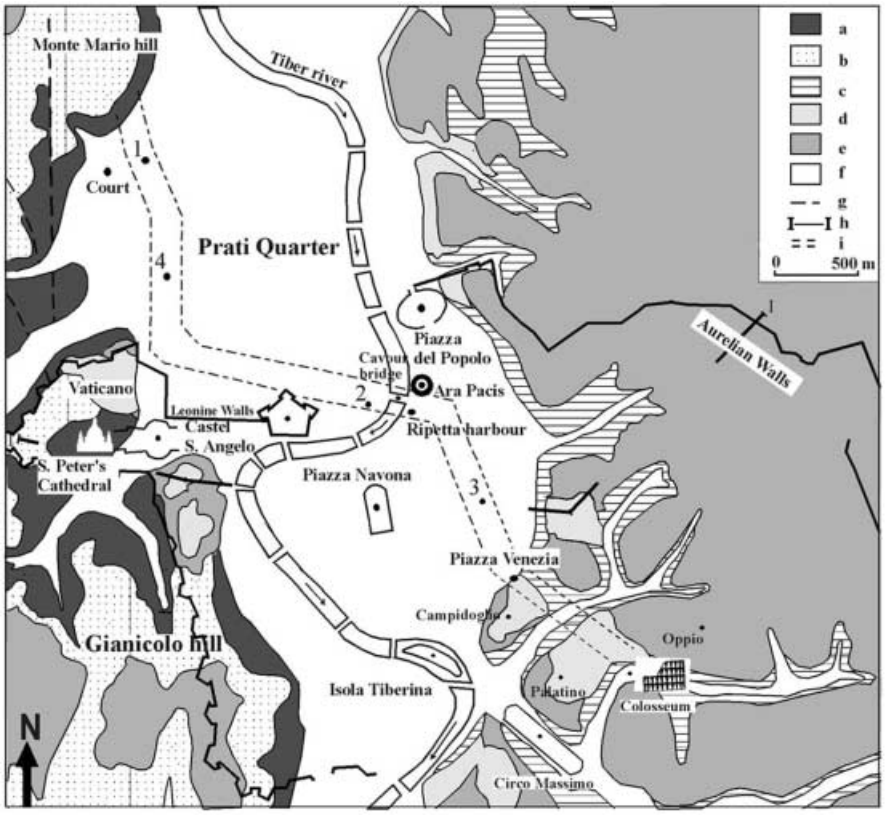

Fig. 3
Geological map of historical centre of Rome: *a* Monte Vaticano Unit (Middle to Upper Pliocene); *b* Monte Mario Unit (Lower Pleistocene); *c* Paleo Tiber Unit (Middle Pleistocene); *d* synvolcanic Unit (Middle to Upper Pleistocene); *e* Volcanic Unit (Middle to Upper Pleistocene); *f* Recent alluvium (Holocene to present); *g* inferred faults; *h* trace of section "I-I" shown in Fig. 4; *i* trace of section shown in Fig. 9 with location of four boreholes. Note: anthropic fill material is not considered in this map. (Modified from Marra and Rosa 1995b)

The marine units described above were deposited in wide depressions created by extensional tectonics linked to the opening of the Tyrrhenian Sea (Fig. 5). Beginning in the Upper Miocene, these events caused the dislocation of the Mesozoic-Cenozoic units which were previously involved in the Apennine orogenesis. The marine deposits can be correlated with three principal marine cycles related to eustatic oscillations, with the first forming the Monte Vaticano Unit during the Middle-Upper Pliocene and the second and third cycles forming the Monte Mario and Monte delle Piche Units during the Lower Pleistocene (Marra and Rosa 1995a). The sediments associated with these last two cycles have sedimentary characteristics which are different to those of the first, indicating a decrease in the depth of the basin. This difference is due to the progressive westerly migration of the coastline during the slow uplift of the area behind the present Tyrrhenian coast, a region in which fluvial-palustrine facies were deposited in a continental environment up until the end of the Lower Pleistocene. These continental sediments were carried by the paleo-Tiber and its tributaries during several depositional cycles (Faccenna et al. 1995). Two principal, Middle-Pleistocene fluvial cycles recognised within the city can be correlated with different positions of the paleo-Tiber river bed and mouth, with deviations in the river's course being caused by tectonics which activated north west/south east trending faults. The first cycle is reputed to have resulted in the formation of the "Ponte Galeria Unit" (Paleo-Tiber Unit 1), whose deposits are found predominantly in the south west surroundings of Rome (Marra et al. 1998). The sedimentary succession represents different phases of a complete transgressive cycle, beginning with fluvial sediments and ending with back-basin sands. A contrary view put forward in recent studies (Milli 1997) is based on sequence stratigraphy analysis and defines the "Ponte Galeria Sequence" as the depositional sequence covering the time interval corresponding to Middle–Late Pleistocene to Holocene with a different depositional

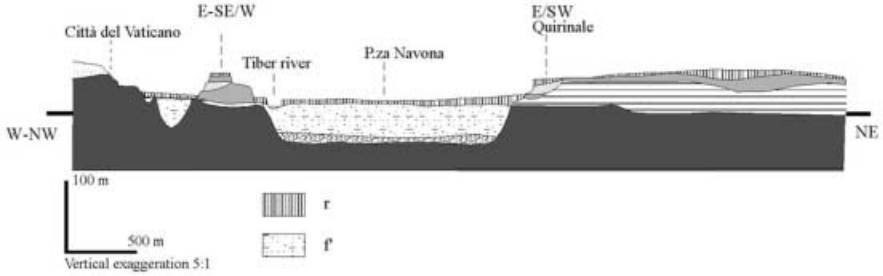

Fig. 4
Geological section across the Tiber River valley (line "I-I" in Fig. 3). Lithologies are generally as described in Fig. 3 but *f'* Recent alluvium (Holocene to Present); *r* anthropic fill material. (Modified from Marra and Rosa 1995b)

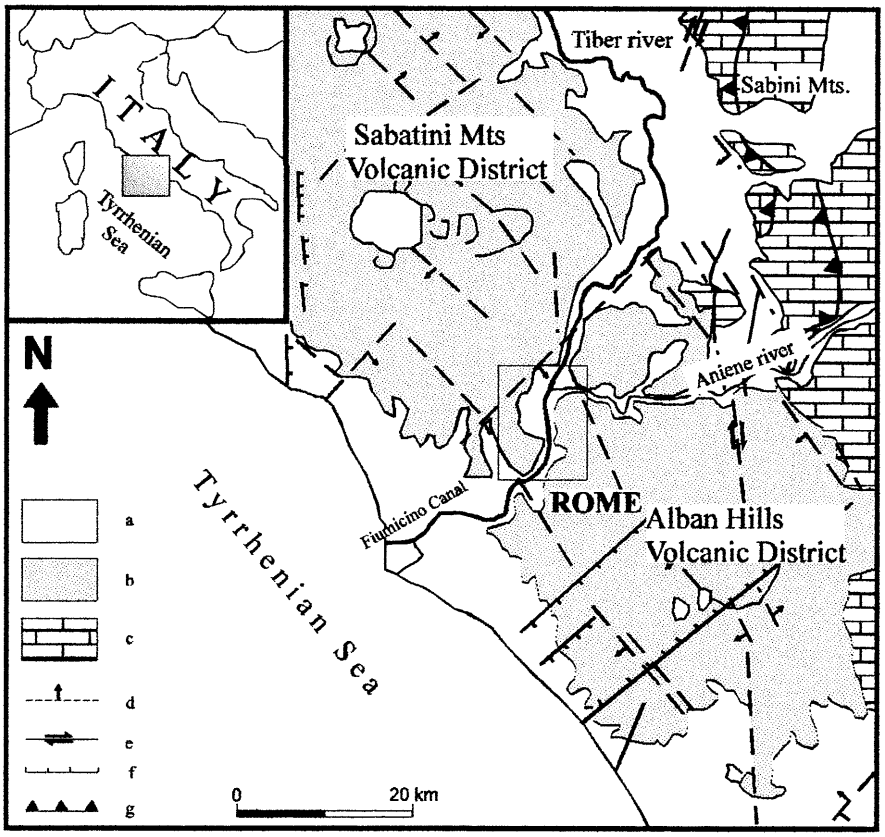

Fig. 5
Geological map of the area surrounding Rome: *a* Messinian to Holocene sediments; *b* Pliocene-Pleistocene lavas and volcanoclastics; *c* Mesozoic to Cenozoic sediments; *d* main buried faults (*arrows* indicate the lowered side); *e* transcurrent faults; *f* normal faults; *g* thrust faults. (Modified from Sagnotti et al. 1994)

system. The deposits of the second cycle, which are predominantly located in the historical centre of the city, are known as the "Paleo-Tiber Unit 2" (Marra and Rosa 1995a) and consist of a basal gravel horizon above which are lacustrine clays and fluvial-palustrine sandy clay deposits. For reasons of clarity, Paleo-Tiber units 1 and 2 have been combined in the geological map presented in Fig. 3.

Pyroclastic deposits (Fig. 5) erupted by the SMVD (30 km north west of Rome) and the AHVD (25 km south east of Rome) overlie the sediments described above. This predominantly explosive, alkaline-potassic volcanic activity initiated during the Middle Pleistocene (614 ± 3 ka for the SMVD and 557 ± 14 ka for the AHVD; Karner and Marra 1998) and is likely to have concluded at the end of the Upper Pleistocene. The dating of the last eruption of the AHVD is not known (Voltaggio et al. 1994). The significant quantity of pyroclastic flow and fall deposits emitted during this period greatly modified the morphology of the Rome area and confined the paleo-Tiber in its present course. In particular, the hills of Monte Mario, Vaticano and Gianicolo formed a barrier to the pyroclastic flows which travelled north eastwards from the AHVD and south eastwards from the SMVD.

Continental sedimentary units located at the borders of the present Tiber River valley were deposited in cycles controlled by eustatic variations during the emplacement of the principal pyroclastic flows. These sediments, known as the Valle Giulia, S. Paolo and Aurelia Units, are grouped together in Fig. 3 as a syn-volcanic unit. They are generally characterised by fluvial-lacustrine deposits which include reworked volcanic material and which have complex stratigraphic relationships with the different volcanic units. The urban area of Rome is therefore characterised on the left bank of the Tiber River alluvial plain by volcanic products in direct contact with the continental deposits of the paleo-Tiber and on the right bank almost exclusively by marine Pliocene–Pleistocene deposits (Figs. 3 and 4).

This geological setting is linked to important tectonic movements which occurred contemporaneously with and subsequent to marine sediment deposition, along NW–SE, NE–SW and N–S trending faults systems which isolated the Monte Mario–Vaticano–Gianicolo Ridge and lowered the historical centre area. The last of these was active primarily during the Middle–Upper Pleistocene. In addition, erosion linked to a marine regression following the deposition of the Ponte Galeria Unit removed the previously deposited Pleistocene-aged sediments. As a consequence, the Lower Pleistocene sediments are absent on the left bank of the Tiber River in the area of Rome (Fig. 4) and the Middle Pleistocene continental deposits (Paleo-Tiber unit 2) are in direct contact with the erosional surface of the Pliocene substratum (i.e. the Monte Vaticano Unit).

Recent geological evolution of the area of Rome

The most important recent event which has affected the present geological and morphological setting of the Rome area is the marine regression associated with the last

glacial maximum (i.e. *Würm*) dated at around 18,000 years b.p. (Chappel and Shackleton 1986). This event was responsible for the lowering of the sea level by more than 120 m with respect to the present level and, as a consequence, the erosion of hydrographic networks such as that of the Tiber River. For example, in the presently urbanised area the Tiber riverbed cut a channel into the Pliocene substratum to a depth of –50 m relative to the modern sea level, forming a wide valley more than 60 m deep with sloping river banks and a flat thalweg. The subsequent sea level rise between 18,000 years b.p. and today caused drastic changes including the modification of the Tiber River base level. This resulted in a significant retreat of the river outlet and the related depositional zone.

Studies conducted on the Tiber River delta (Belluomini et al. 1986; Bellotti et al. 1995) indicate that sea level rise in this area was episodic rather than constant, with phases of stability alternating with periods of rapid rising until the sea level stabilised at the present level about 5000 years ago. From 18,000 to 10,000 years ago the rise in sea level appears to have been rapid and discontinuous (13 mm/year), becoming successively more gradual between 10,000 and 5000 years ago (5 mm/year). This sea level rise was likely to have been accompanied by at least eight stable phases, of which the last (0 m above present sea level) began 5000 to 4700 years ago.

The sea level rise curve constructed for areas beyond the Tiber River delta (Alessio et al. 1992) indicates a rapid rise from –9.5 to –3.5 m a.s.l. between 6770 and 6500 years b.p. Sea level continued to rise until it reached approximately present-day level between 6000 and 4000 years ago, during the *Optimum* (warmest post glacial time) when the climate was relatively hotter than the present day (Pinna 1977). Around 3500 years b.p. the level dropped by some 2 m before rising again to its present-day level.

Based on reconstructions made in the Tiber delta area (Bellotti et al. 1997) it is believed that 18,000 years ago the river outlet occurred approximately 10 km to the west of its present location. Around 12,000 years ago, when the sea level was around –70 m below the present level, the Tiber valley terminus was invaded and the river outlet was repositioned within a coastal lagoon that extended along the axis of the valley (Fig. 6a). During this phase the river deposited a large part of its load further upstream in the interior of the alluvial valley, transporting only small quantities of predominately fine material to the river outlet. About 10,000 years ago the rate of sea level rise significantly decreased (sea level was at –30 m with respect to present level), resulting in a change in the fluvial regime and a related increase in the solid load to the river outlet. With the most recent sea level rise between 7000 and 5000 years ago the Tiber River outlet withdrew into the valley interior for the last time and the lagoon was positioned parallel to the coast (Fig. 6b, c). Around 5000 years ago (Fig. 6c) the river outlet began to prograde rapidly into the lagoon, filling this structure step-wise until it eventually reached the coast. Although the precise age of this event is still unknown, it is certain that during the Imperial Roman period (around 1800 years ago, Fig. 6d) the Tiber had already initiated the present marine-delta phase which divided the old lagoon into two wide marshy areas.

The progradation of the Tiber delta over the last 2000 years is clearly shown by the distribution of various historical buildings. For example, the ancient city of Ostia (which was originally founded on the coast by Anco Marzio in 633 b.c.) and the Harbour of Claudio (built originally in 42

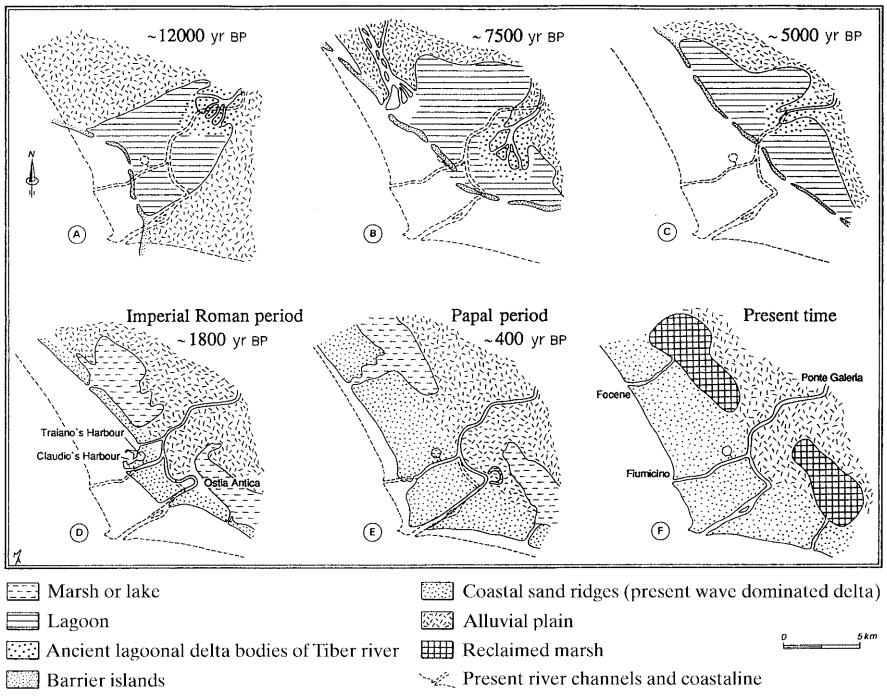

Fig. 6
Paleogeographic sketches showing evolution of the Tiber River downstream of Rome. (Reproduced from Fig. 9, Bellotti et al. 1995)

a.d.) are both presently located approximately 3 km from the sea (Fig. 6d). Furthermore, the position of some watch towers constructed during the Papal period (around 400 years ago, Fig. 6e) and maps from the last two centuries indicate that the progradation of the delta was not constant. In fact, data indicate that erosional and depositional phases alternated during the Middle Ages and that progradation only became continuous from the sixteenth to the twentieth centuries. This variable progradation velocity has been attributed by some authors (Oberholtzer 1875; Belluomini et al. 1986) to the opening of a second outlet, the Fiumicino Canal, by Traiano during the Imperial epoch (Fig. 6f). This waterway eventually fell into disuse, but was reopened at the end of the sixteenth century a.d. and is presently still functioning.

With regard to the ≤ 60 m thick succession of sediments deposited within the urbanised area of the Tiber River valley and its tributaries since the last glacial low-stand, available data (Gigli 1971; Ventriglia 1971; Amanti et al. 1995; Marra and Rosa 1995a; Bozzano et al. 1997) indicate the presence of an ~ 10 m thick basal gravel unit and a more extensive overlying horizon of clayey-silty and sandy-silty sediments with peat intercalations (Fig. 4).

On the basis of this knowledge and considering the models proposed for the filling of other large alluvial valleys by rising sea levels (e.g. Weimer 1986; Miall 1996), it is reasonable to hypothesise that the Tiber River initially formed a braided stream in the area presently encompassed by the city of Rome. The basal gravel would have been deposited during this phase – as river energy decreased, the majority of its coarse load would have been deposited in the alluvial valley and only a small amount of predominantly fine materials would have been transported to the river outlet. Subsequently, the Tiber River began to meander, the sinuosity index progressively increased and fine-grained overbank deposits were developed.

More recent information regarding the course of the Tiber River in this area can be obtained from historical sources of the Roman epoch. At the time of the founding of the city of Rome (eighth century b.c.) the morphology of the area was very irregular. The left bank of the Tiber River was quite hilly, with the famous seven hills of Rome (consisting of volcanic deposits) stretching from the NE to SW towards the Tiber (Fig. 7). In contrast, the right bank was and is still dominated by the ridge joining the hills of Monte Mario, Vaticano and Gianicolo with its very steep slopes of Pliocene–Pleistocene marine deposits. A tight network of fluvial incisions formed within the hills of both the right and left banks (the paleo tributaries of the Tiber), while vast swampy and marshy areas developed near the Tiber River itself. During the Renaissance these urban area morphologies were in part still present, although they are less obvious today due to successive filling.

Detailed bibliographic documentation indicates that the Tiber River was subject to frequent and dangerous floods and, even today, rare ancient tablets can still be found in some city districts along the river which indicate the levels to which the floods reached (Ravaglioli 1998). A total of 46 serious floods have been documented for the period 414 b.c. to 1870 a.d., of which the most damaging appear to have occurred in 1598 a.d. and 1870 a.d. (Bencivenga et al. 1995). Numerous attempts were made to eliminate or reduce this danger, but it was not until work following the 1870 event that the risk of flooding to Rome was essentially eliminated. This work, undertaken between 1876 and the early 1900s, involved the construction of "muraglioni" (high walls) along the entire length of the Tiber River within the city limits and interventions on the upstream portion of the basin. Today, some 35% of the historical centre, which contains the most important historical monuments, as well as other areas of more recent development to the north west and south of the city are built on

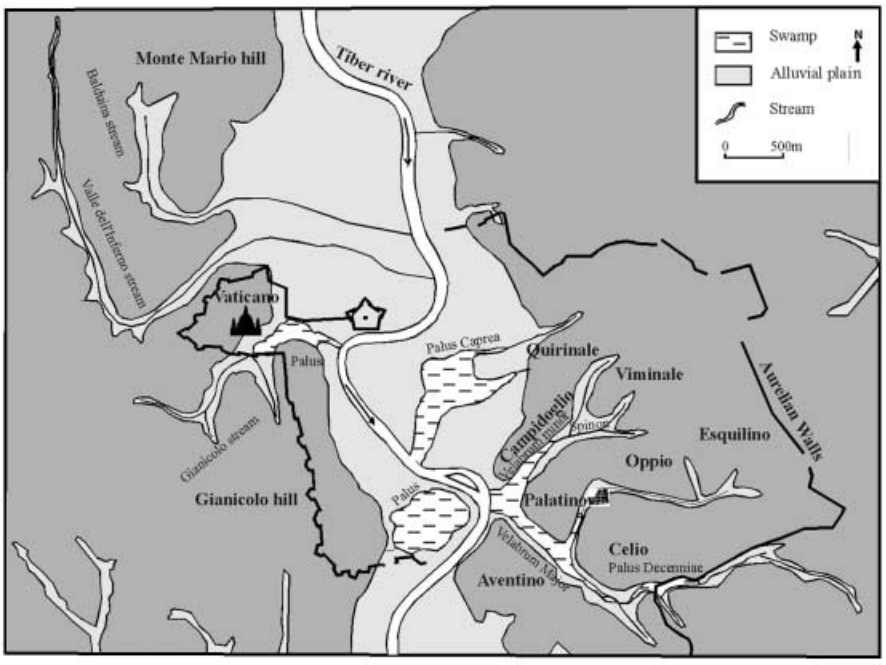

Fig. 7
Ancient hydrology of Rome. (Modified from Corazza and Lombardi 1995)

recent sediments of the Tiber River and its complex tributary network.

Reconstruction of a section of the Tiber River alluvial body within the city of Rome

The Tiber valley fill sediments were examined in detail along a 5.5 km long NW-SE section (see Fig. 3) which begins at the foot of M. Mario hill to the north, passes through the Prati quarter, crosses the Tiber River at the Cavour bridge (near the Ara Pacis) and the ancient part of the historical centre through Piazza Venezia before passing out of the recent alluvial plain and onto the slopes of the hills of Campidoglio, Palatino and Oppio and terminating at the Colosseum to the south east. In general, the section is either subparallel or oblique to the trend of the Tiber River valley; only in the middle section is it approximately perpendicular. In addition, the southern part of the section cuts the valley of a paleo tributary of the Tiber River (Fig. 7).

The geological reconstruction of this section was based on data collected from 57 continuously cored boreholes which were uniformly distributed within the belt delimited in Fig. 3. These boreholes, which range in depth between 30 and 67 m b.g.l., penetrate through the sediments filling the Tiber River valley and, in numerous cases, terminate in the Pliocene substratum (i.e. Monte Vaticano Unit).

The logging of these drill cores has highlighted the vertical and lateral variability of the lithologies that fill the Tiber River valley, as shown in the examples in Fig. 8. This variability was reduced to seven lithotypes based on the following criteria:

- Lithotype G: predominantly limestone gravel in a grey, sandy-silty matrix.
- Lithotype D: alternating silty-sandy, sandy-silty, clayey-silty and clayey levels. Viewed together, this unit is grey in colour.
- Lithotype C: grey clay and silty clay with a variable organic content that gives a local black colour. Occasional up to 100 mm thick peat levels and rare sandy silt layers with gravel are also present.
- Lithotype B: brown to yellow (more rarely grey) coloured, sandy and silty-sandy sediments.
  Lithotype B_1: predominantly yellow-brown, medium- to fine-grained sand and sandy loam; loose or moderately aggregated with pieces of wood or plant material.
  Lithotype B_2: alternating layers of sandy and clayey loam varying between yellow and grey in colour.
- Lithotype A: silty and sandy deposits with brick fragments identified with the *historical alluvium*.

Fig. 8
Simplified logs of three boreholes (for borehole location see Figs. 3 and 9)

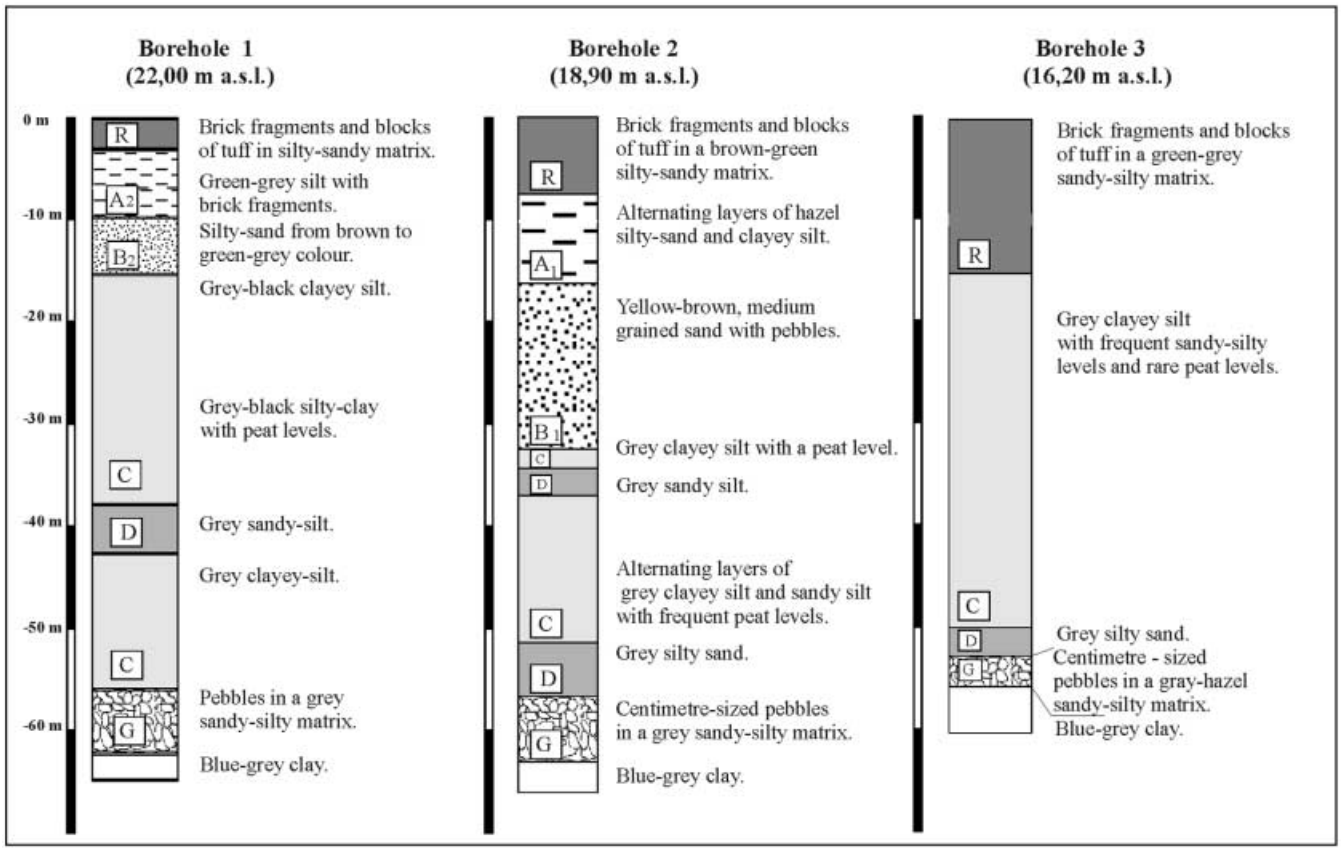

Lithotype A_1: green-grey silty sand and silty loam.
Lithotype A_2: hazel-coloured clay and clayey silty bands which contain organic matter and black-brown pyroclastics.

- Lithotype R: anthropic fill material characterised by abundant, variously sized brick fragments and blocks of tuff embedded in a brown-green silty-sandy matrix. This horizon also contains ceramic and mortar fragments.
- Lithotype Dv: slope detritus located near the scarp of the Tiber paleovalley. On the right bank it consists of brown-green, silty, sandy and locally clayey material, while on the left bank brown and grey, coarse-grained sand has been found (at the foot of the paleoscarp) to overlie a 5 m thick block of lithoid tuff which is probably related to a paleo-landslide body.

Based on these subdivisions the 57 boreholes have been correlated and the resultant lithostratigraphic section provided in Fig. 9. Attention is drawn to the significant vertical exaggeration in this figure, as illustrated by the fact that both valley walls have an average slope of about 14°. It can be seen that the base and right slope of the principal valley are cut into the Monte Vaticano Unit, while along the left bank, to the south east of Piazza Venezia, the Pleistocene-aged Paleo Tiber and Valle Giulia Units are also present.

The bedrock erosional surface on which the alluvial sediments are deposited is almost horizontal and is found at an average elevation of around –45 m a.s.l., resulting in an overlying sediment thickness of about 60 m. A local depression of this surface is hypothesised in the area of Piazza Venezia.

Lithotype G (basal gravel) was found uniformly above the erosional surface, with an undulating upper surface and a thickness ranging between 2 and 10 m. Clay and silty clay (lithotype C) are deposited above this basal gravel and form the major part of the alluvial fill. Except for some northern parts of the valley where lithotype C is in direct contact with the basal gravels, the transition from lithotypes G to C mainly occurs via the gradual placement of the silty-sandy and sandy-silty levels ascribed to lithotype D.

On the right bank of the present Tiber River, towards the interior of lithotype C, there are lateral heteropic bodies consisting of alternating sandy-silty, clayey-silty and clayey layers (lithotype D). These bodies occur as lenses where the section is transverse to the Tiber River valley. Where the section is subparallel to the valley, however, the geometry is rather irregular and difficult to resolve on the basis of the available borehole data; a possible solution is presented in Fig. 9. In contrast, lithotype C occurs as an almost continuous unit on the left bank of the present Tiber River and has a total thickness of around 50 m.

The sands and sandy loams of lithotype B_1 and the sandy loams and clays of lithotype B_2 overlie lithotype C along sharp, undulating contacts. Their complex geometry is generally lenticular in transversal section but becomes tabular near the northern slope of the valley, the upper surface being weakly undulating. Lithotype B_1 characterises the central part of the section near the present Tiber riverbed and grades laterally to the north into lithotype B_2. Both units reach up to 20 m in thickness, although lithotype B_2 thins towards the northern border of the valley. In contrast these units are essentially absent towards the south in the area of Via del Corso–Piazza Venezia, although lithotype B_2 is observed to fill a paleo-tributary valley (25 m thick) on the south side (Spinon stream, Figs. 7 and 9).

The silty sand and silty loam of lithotype A_1 and the clay and clayey silty deposits of lithotype A_2 occur above lithotypes B_1 and B_2 in the centre and north of the section and above lithotype C in the south. Lithotype A_1 is found in correspondence with the present-day trace of the Tiber River, heteropically grading to the north and south into lithotype A_2. In general, lithotype A_2 is thinner and less continuous on the left bank of the river than on the right, where it reaches a maximum thickness of 15 m.

The anthropic fill material which forms lithotype R and represents the most recent sediments overlies lithotypes A_1 and A_2 and, on the southern border of the valley, lithotype C. It is also found along the section outside of the valley above the paleo Tiber and Valle Giulia Units. The average thickness of this unit is between 7 and 8 m, with the higher values occurring on the left bank of the river in correspondence with the ancient part of the historical city centre. An exception to these average values occurs near the "muraglioni" forming the embankment of the Tiber River around the ancient Porto di Ripetta (Figs. 3 and 9), where lithotype R reaches a maximum thickness of 22.5 m. Such a unique case is probably linked to the presence of the ancient harbour as it was built at the beginning of the eighteenth century and then subsequently demolished for the construction of the previously mentioned muraglioni and the Cavour bridge (Insolera 1980). On the right bank of the Tiber River the thickness of lithotype R gradually diminishes to about 3–4 m on the slopes of M. Mario. Finally, a unit consisting of slope deposits, lithotype Dv, has been inferred on the basis of data from three boreholes drilled along both valley walls. The geometry and extent of this unit is clearly somewhat simplified due to the limited amount of data available.

Geological interpretation of the section

The lithological section proposed in Fig. 9 provides information regarding the evolution of the Tiber River and its alluvial plain relative to the time interval between the end of the Würmian regression (which represents the start of the infilling of the valley some 18,000 b.p.) and the present. The occurrence of gravel deposits (lithotype G) at the base of the alluvial succession implies that the Tiber River was initially a braided stream, whereas the transition to the finer sediments of lithotypes D and C indicates that it progressively became more meandering with the presence of vast palustrine areas. In particular, the vertical

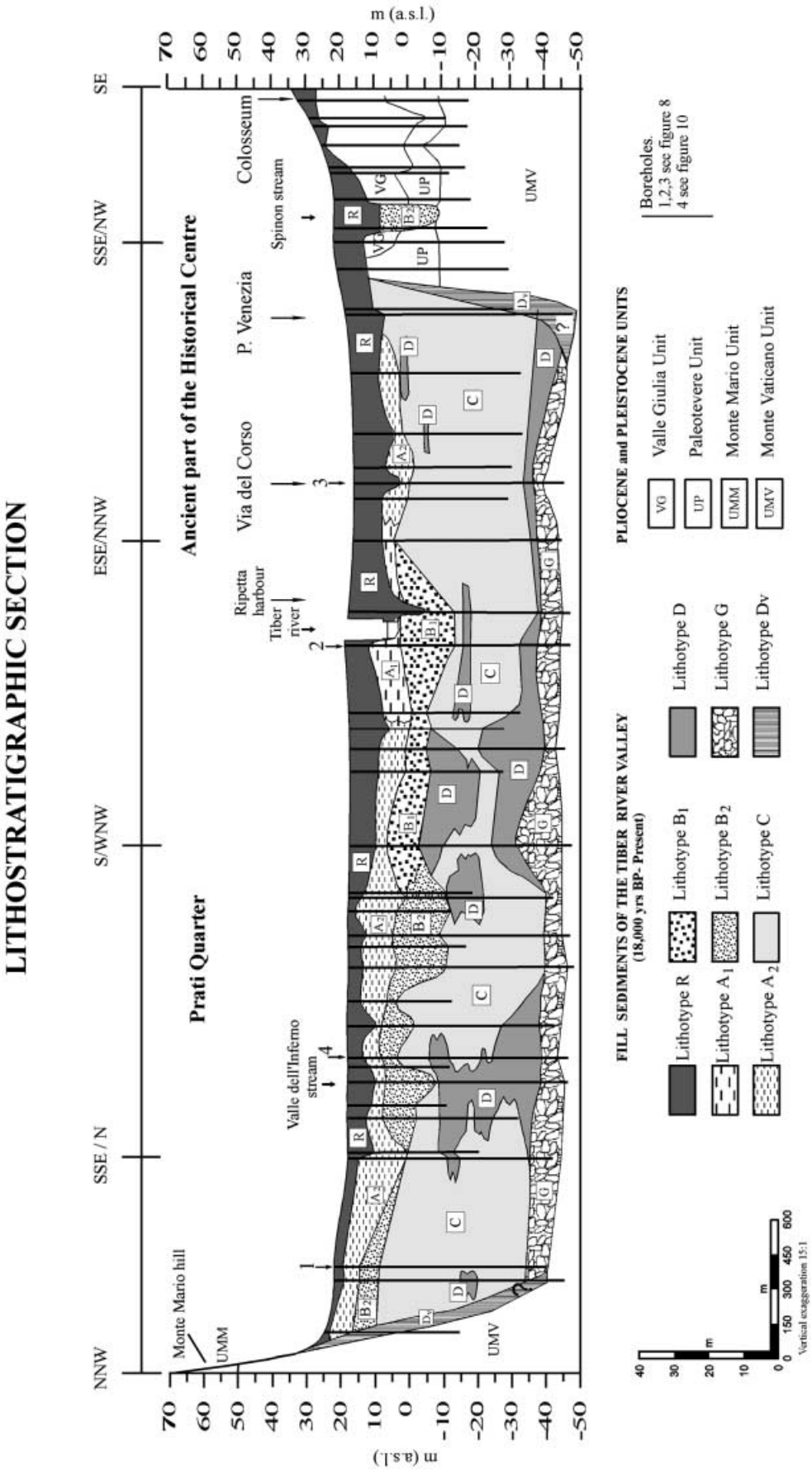

Fig. 9
Lithostratigraphic section across the Tiber River alluvial plain (for borehole location see Fig. 3)

continuity recognised for lithotype C on the southern side of the section, coinciding with a large part of the ancient part of the historical city centre, implies the continuous presence of a palustrine environment which was located at the margin of an important waterway which periodically flooded. The existence of this type of depositional environment is confirmed by historical sources only from the third to second centuries b.c. onwards (see Corazza and Lombardi 1995). These sources report the occurrence of small lakes and swamps in this area, such as Palus Caprea, Velabrum Major and Velabrum Minor (Fig. 7), as well as periodic alluvial activity.

On the northern side of the section the lateral heteropic relation between the alternating silty-sandy, sandy-silt and clay levels of lithotypes D and C indicates the almost continual presence of tributaries between 18,000 b.p. and the present, defining an alluvial floodplain which was formed not only by the main Tiber River but also by its right bank tributaries. Based on this hypothesis, lithotype D may represent the deposits in correspondence with and near the riverbeds, including the principal one, while lithotype C represents those between the river beds. The historical pathways of the Tiber River and its tributaries within the city of Rome are, however, only known with sufficient certainty from the seventeenth century a.d. onwards (Contini 1661), whereas before this date only general references exist. It can be said, however, that the Valle dell'Inferno stream (Fig. 7), whose trace has largely been cancelled by present-day urbanisation, was clearly evident until the end of the last century (Cipriani 1830) and it represents an example of the more recent evolution of the Tiber River tributaries which have left geological evidence in the form of lithotype D sediments located on the northern side of the section in Fig. 9.

The grain-size and compositional changes which occurred in the sediments beneath Rome due to the change from lithotype C to B (Fig. 8) indicate that the hydraulic regime of the Tiber River must have undergone a significant change subsequent to the events described above. The radiometric C^{14} dating of some organic matter present in the sediments (Stuiver and Reimer 1993) places this event between 9500 and 3000 years b.p. (Fig. 10), which is in good agreement with a progradation of the Tiber River delta starting at around 5000 years b.p. and continuing during present times (Bellotti et al. 1997). The irregular basal contact of lithotypes B_1 and B_2 and the related geometry of these bodies, which mimic the filling of valley depressions, imply erosional activity with the partial reincision of the alluvial body and successive filling of valleys.

The irregular setting of the alluvial deposits above the B–C contact characterises the zone below and near the present Tiber River channel. Whilst this type of geometry is clearly evident on the right bank in correspondence with the Balduina and Valle dell'Inferno streams (Fig. 7), it is not found on the left. This difference implies that the course of the Tiber River (lithotype B_1) and the network of the principal tributaries of the right bank (lithotype B_2) were well developed within the alluvial plain, whereas the stream network on the left bank was less well developed, at least in the area crossed by the section. This is shown by the larger amplitude and by the steeper gradients of the hydrographic basins of the right-bank tributaries (Figs. 7 and 11). Furthermore, on the southern side of the section (outside the Tiber River valley), is an incision filled by alluvial deposits attributed to the Spinon stream, which carries water from the hills of Quirinale, Viminale and Esquilino (Fig. 7). This indicates that a tributary network is also evolving on the left bank from the gentle slopes facing the Tiber River alluvial plain. It is probable that on reaching the Tiber River alluvial plain (Fig. 7), these tributaries are dispersed to the interior of the palustrine area.

As lithotype B_1 has a larger grain size than B_2, it is likely that currents along the principal channel had a higher energy than those in the tributaries. The fact that the

Fig. 10
Interpretation of absolute dating results (for borehole location see Figs. 3)

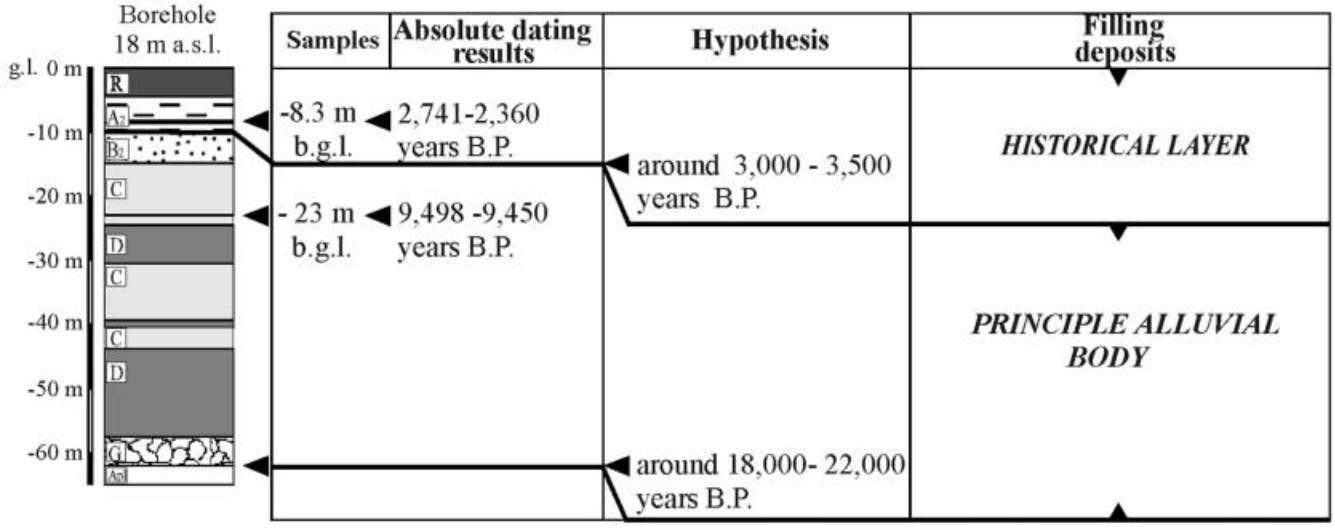

Fig. 11
Layout of Rome and its surroundings as drawn by Ufficiali di Stato Maggiore Francese (1868)

present course of the Tiber River in the Rome area (Fig. 9) is not centred with respect to the main B_1 body suggests that it had a different trend. It would be anticipated that this would have been more rectilinear during the period of change described above, subsequently becoming more meandering in response to the rapidly decreasing rate of sea level rise and eventual stabilisation. However, the good correspondence on the northern side of the section between depressions in the upper surface of lithotype C filled by B_1–B_2 sediments and the trace of the Valle dell'Inferno stream (Figs. 7 and 9) implies that the position of the right bank tributaries has remained nearly stable from the erosive event to recent times.

The vertical transition from lithotypes B_1–B_2 to the relatively finer-grained A_1–A_2 indicates a progressive decrease in the transport capacity of both the principal river and its tributaries. The lithological variation between lithotype A_1 (located around the principal riverbed) and A_2 (further away) is probably due to the same reason on postulated for the difference between lithotypes B_1 and B_2.

The presence of human artefacts within lithotypes A_1 and A_2, including fragments of ceramics, marble, cemented mortar and building stones, implies that this hypothesised change in the hydraulic regime of the Tiber River occurred during historic times (around 3000 years b.p.), an interpretation that is supported by carbon-dating results (Fig. 10).

The variations in thickness of lithotypes A (A_1 and A_2) and R on the right and the left banks of the Tiber River (Fig. 9) almost compensate each other if their summed total thickness is considered. In other words, it appears that the deposition of alluvial sediments on the right bank was contemporaneous with that of the anthropic detritus on the left – an interpretation that is supported by what is known regarding the urbanisation of the area. The Prati quarter of Rome, on the northern side of the section, was covered by gardens, vineyards, yards and sporadic building from Roman times to the beginning of this century, whereas the southern zone represents the ancient historical centre of the city and was heavily and continually settled during the same period (Fig. 11). The northern zone was periodically flooded by the Tiber River, as shown in recent times both before 1870 and during the building of the river embankment (between 1876 and the early 1900s). In contrast, the flood deposits found in the historical centre were mixed with large quantities of anthropic fill material. This material has been accumulating for at least 2000 years and was used to reclaim swampy areas and to reduce the dangerous effects of the flooding.

An example of this was seen in the excavations in the left bank of the Tiber River. These uncovered the ancient Via Lata (corresponding to the present-day Via del Corso which joins Piazza del Popolo with Piazza Venezia – Fig. 3) at a depth of 5.3 m and another pavement level consisting of lava cobble-stones at 6.4 m below the present ground surface. These levels can be considered in terms of the soil accumulated from the first Republican age (fifth to first century b.c.). The 6.4 m level was constructed before the age of Augusto (63 b.c. to 14 a.d.) while the 5.3 m level is the average elevation the road attained as a consequence of the build up of soil in the Campo Marzio marshy area associated with the land reclamation work of Adriano (76–138 a.d.) using the remnants of the famous Fire of Nero (Lugli 1961).

In a similar manner, the discovery of the remains of a Roman road and ancient circus (*Circus Gai et Neronis*) on the right bank of the Tiber River makes it possible to estimate the beginning of soil accumulation caused primarily by flooding. The Roman block paving was discovered at the slopes of M. Mario, near the city's judicial building (noted as Court in Fig. 3) and has been identified as part of the ancient Via Triumphalis which has also been discovered in other parts of the city. The Roman road occurs 4 m below the base of an adjacent building which can been used as a reference point. In view of its location near the Tiber River and the fact that the block-paving is of Imperial age, it is likely the 4 m difference is related to alluvial material deposited in the last 2000 years.

The remains of the ancient circus (1 a.d.) are also a good indicator of soil accumulation due, at least in part, to flooding. This structure was discovered during excavations for the foundation of Saint Peter's Cathedral (sixteenth and seventeenth centuries a.d.); the basilica was positioned with the same E-W orientation as the circus, with the left aisle coincidence with the longer northward side and the obelisk located in the centre. It is possible to estimate some 13 m of soil accumulated in this area (Gigli 1971).

Hydrogeological conditions within sediments filling the Tiber River valley

The hydrogeological analysis was based on an interpretation of water-level data obtained from both Casagrande piezometers and open tube piezometers installed in some of the boreholes drilled along the section together with permeability data for the different lithotypes and background literature information.

The base of the local hydrogeological system is formed by the clayey Pliocene sediments of the Monte Vaticano Unit, which act as a very low-permeability ($k = 10^{-10}$ m/s) substratum throughout the entire Rome area. The principal aquifer of the area occurs in the basal gravel (lithotype G), with flows towards the south of the highly mineralised water (Corazza and Lombardi 1995) occurring from a recharge area north of Rome. Piezometric head values range between 9 and 10 m a.s.l.

In the overlying alluvial deposits it is possible that bodies of lithotypes B and D ($k = 10^{-6}$ and 10^{-7} m/s respectively) may represent local aquifers within the low-permeability lithotypes A and C ($10^{-6}/10^{-8}$ and 10^{-10} m/s respectively). Piezometric data confirm the existence of this layered aquifer/aquiclude system (average water level 15 m a.s.l.), with the general water flow likely to be towards the Tiber River. This framework is more complicated on the north

side of the section due to the presence of more frequent, relatively coarser levels (lithotypes B and D). It is probable that the nearby hills provide the recharge for these aquifers, at least since urbanisation of the alluvial plain began to impede direct infiltration. Regarding the connections with the Tiber River, the aquifer within lithotype B_1 appears to feed the river when the Tiber is in a low to normal flow regime, but during high flow periods the gradient is reversed and the river recharges the aquifer.
Data regarding the surface anthropic fill sediments indicate an unconfined aquifer bounded by a low permeability base formed of lithotypes A and C. Given the high level of urbanisation in the area, this aquifer is more likely to be fed by loss from the sewer and aqueduct systems and/or by ancient, buried springs than by direct infiltration.

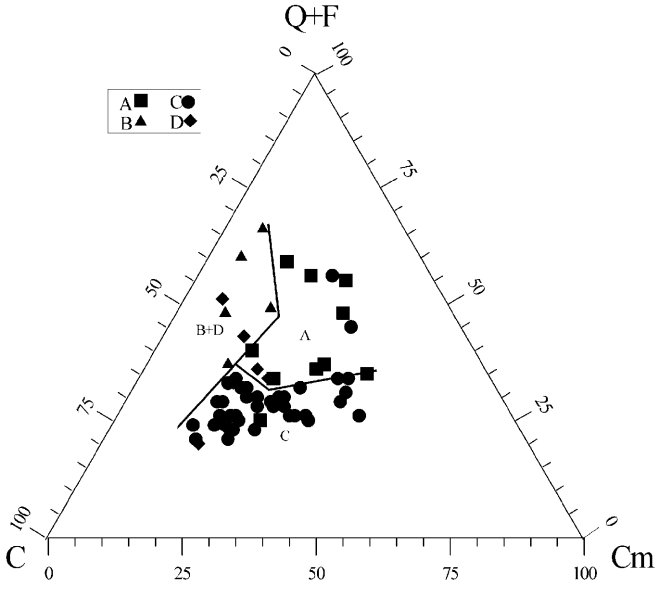

Fig. 12
Mineralogical composition of lithotypes A, B, C and D

Physical and mineralogical characteristics of the Tiber River alluvial deposits

The various deposits that fill the Tiber River valley (lithotypes R, A_1, A_2, B_1, B_2, C, D and G; see Fig. 9) were analysed in the laboratory in order to precisely define their physical and mineralogical characteristics for integration with the macroscopic data outlined above. This characterisation was conducted on samples having medium to high disturbance due to drilling. Granulometric distribution was determined using the Massachussetts Institute of Technology (MIT) granulometric fields and the results plotted on US Bureau of Soils triangular graphs (Rosa 1924). Atterberg limits were obtained following the ASTM standard methods D 422-63 and D 4318-84 (American Society for Testing and Materials 1988) and graphed on plasticity charts using the subdivisions proposed by Casagrande (1948). Semiquantitative X-ray diffractogram (XRD) mineralogical analyses were performed on "whole rock" samples as well as on <2-μm specimens which were either untreated or subjected to ethylene glycol for 8 h at 60 °C. The analyses permitted a discrimination and semiquantitative estimation of the different clay mineral "families" present without addressing details of individual mineral species. The ternary diagram given in Fig. 12 shows the relative abundance of the clay minerals (Cm = mica-like minerals + chlorites + kaolinites + smectites) with respect to quartz + feldspars (QF) and calcite (C), confirming the difference between lithotypes A, C and B-D. In general, the clay minerals consist primarily of mica-like species, with higher quantities of chlorite occurring in only a few samples and very minor amounts of kaolinites and smectites. The organic content was measured using potassium dichromate oxidation of organic carbon in the presence of sulphuric acid (Broadbent 1965).
For lithotypes A_2, B_1, B_2 and C the number of tests conducted and/or the relative homogeneity of the analysed cores means that the data obtained can be considered to be statistically representative, whereas the scarcity and/or heterogeneity of lithotype A_1, D, R and Dv samples means that these results can only be considered as improving the general knowledge of the characteristics of the lithotypes. It should be noted that measurements of mineralogical and organic content were made on what were considered to be representative samples on the basis of their macroscopic lithological characteristics, granulometric distribution, Atterberg limits and activity.

- Lithotype G: The low percentage of core obtained from this predominantly gravelly-sandy lithotype made it of little value for laboratory determinations. A mineralogical analysis of the matrix indicates that clay minerals are absent and that it consists of 90–95% calcite and quartz.
- Lithotype D: This lithotype is characterised by the most variable physical characteristics, reflecting the lithological heterogeneity described above; samples ranged from sand to sandy loam, clayey loam, loam, silty loam, silty-clayey loam, clay and silty clay (Fig. 13a). The fine component is characterised by low to high plasticity (Fig. 13b) and inactivity (activity average value = 0.59). The mineralogical composition consists predominantly of non-clay minerals and, like the physical characteristics, is quite variable; the calcite to quartz + feldspars ratio, for example, varying from 1:1 to 3:1 (Fig. 12). The organic content ($n = 8$ samples) is less than 1%.
- Lithotype C: This unit consists of clay and silty clay (Fig. 14a), having medium and high plasticity (Fig. 14b) with activity from 0.55 to 1.21. Its physical characteristics are generally more homogeneous than those of the other lithotypes, although a detailed analysis of the liquid limit (w_l) and plasticity index (I_p) values in numerous boreholes indicates that these parameters tend to decrease with depth. Above −14 m a.s.l. the average values of w_l and I_p are 68% ($\sigma = 19\%$) and 35%

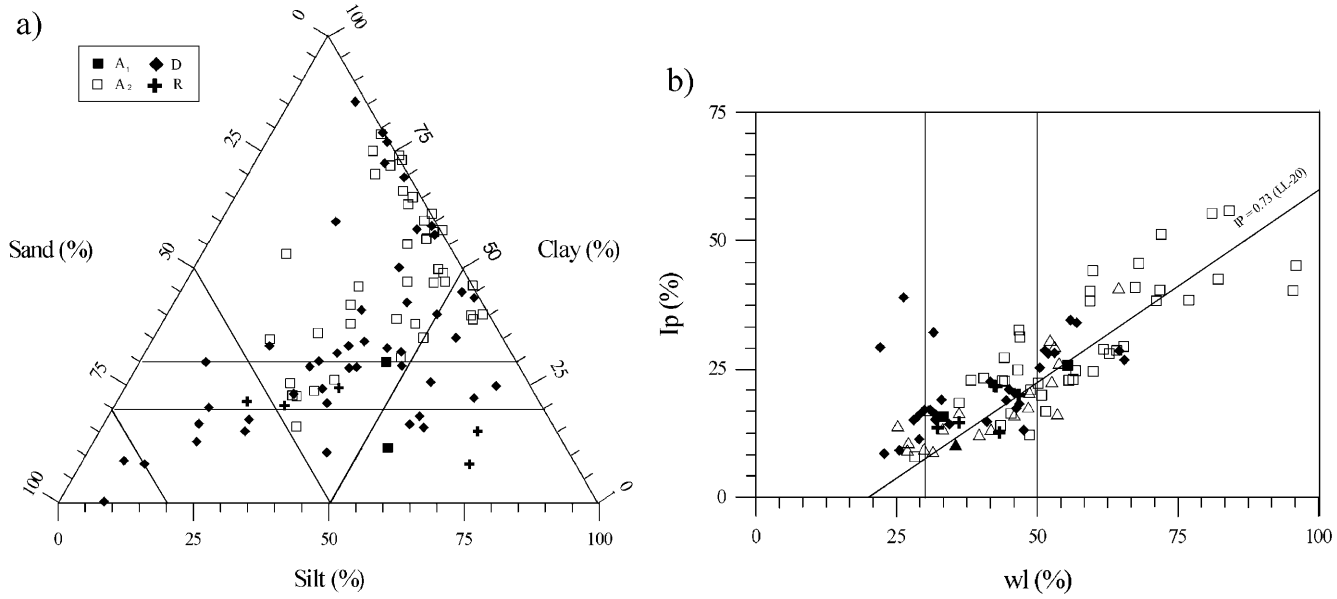

Fig. 13
a Grain size distribution of lithotypes A, D and R; **b** plasticity chart for lithotypes A, D and R

($\sigma = 14\%$), while below this level they are 58% ($\sigma = 14\%$) and 28% ($\sigma = 11\%$). Samples above –14 m a.s.l. (C_1) generally have higher values than those below –14 m a.s.l. (C_2), as illustrated in Fig. 15. This difference in the plasticity limits is not accompanied by significant variations in the granulometric distribution but rather corresponds to a wide variation in the ratio between calcite and clay minerals (Q + F is essentially constant). For example, the average percentage of calcite varies from 35% for group C_1 to 48% for group C_2 (Fig. 16), with an associated change in the C/Cm ratio from 1:3 to 1:1. Furthermore, organically rich, millimetre- to centimetre-thick layers have been observed more frequently above –14 m a.s.l. than below –14 m a.s.l., resulting in C_1 samples having an average organic content of 3.2% (max. = 12.3%) while the C_2 sample average is only 1.4% (max. = 4%). In particular, C_1 clay from the left bank of the Tiber River was always found to have a maximum organic content between –13.8 and –13.3 m a.s.l. whereas C_1 clay from the right bank gave higher

Fig. 14
a Grain size distribution of lithotypes B and C; **b** plasticity chart for lithotypes B and C

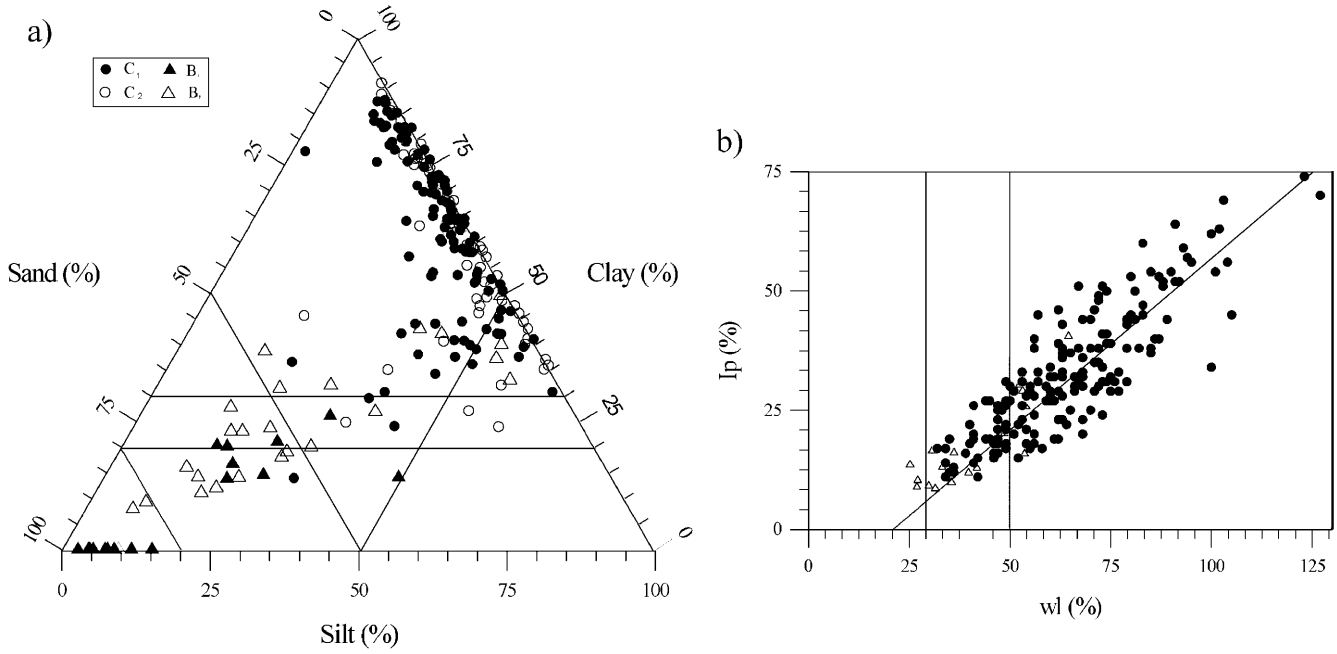

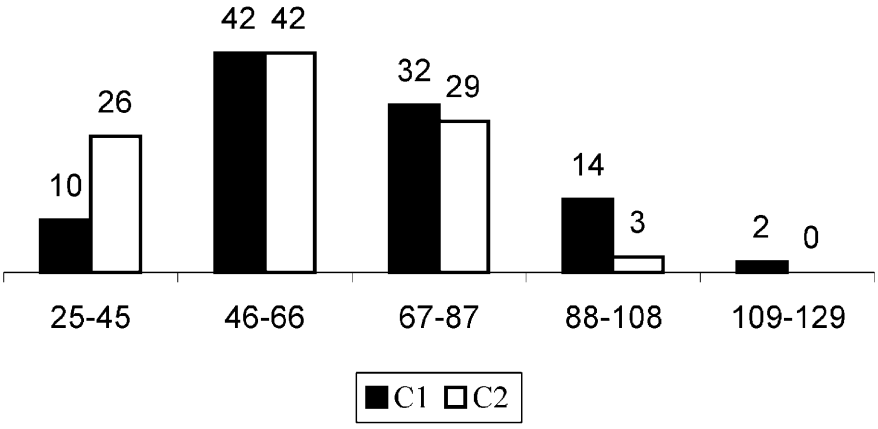

Fig. 15
Distribution of w_l values for lithotype C samples

maximum organic contents at more variable elevations (from –5.5 to +6.8 m a.s.l.). Plotting the liquid limit values indicates that w_l correlates linearly with the total quantity of clay minerals (Fig. 17).

- Lithotype B: The granulometric distribution differentiates lithotypes B_1 and B_2 (Fig. 14a) as the former is characterised by sand, sandy loam and sandy-clayey loam while the latter is predominantly sandy loam, sandy-clayey loam with subordinate silty clay and clay of low to medium plasticity (Fig. 14b). The mineralogical analyses (Fig. 12) show that both lithotypes have an elevated percentage of non-clay minerals ($n=8$; average value = 91%; $\sigma=12\%$) and, as with lithotype D, the ratio C/Q+F varies significantly. The amount of organic matter in lithotype B varies from a minimum of 0.04% to a maximum of 2.1%.
- Lithotype A: The lithological distinction between A_1 and A_2 does not appear to be supported by significant variations in the granulometric distribution, although there were only two samples of A_1 and 41 samples of A_2. This scarcity of data results from the difficulty of distinguishing this lithotype (historical alluvium) from the overlying anthropic unit in the field, especially where the relatively coarser A_1 unit is present. The two samples ascribed to lithotype A_1 are a sandy loam and a clayey loam with medium-high plasticity, while lithotype A_2 is characterised by clay, silty clay and clayey loam which has medium to high plasticity and is inactive or normally active (Fig. 13a,b). In general, the mineralogical composition of lithotype A is quite distinct from that of the other units as it has the lowest recorded

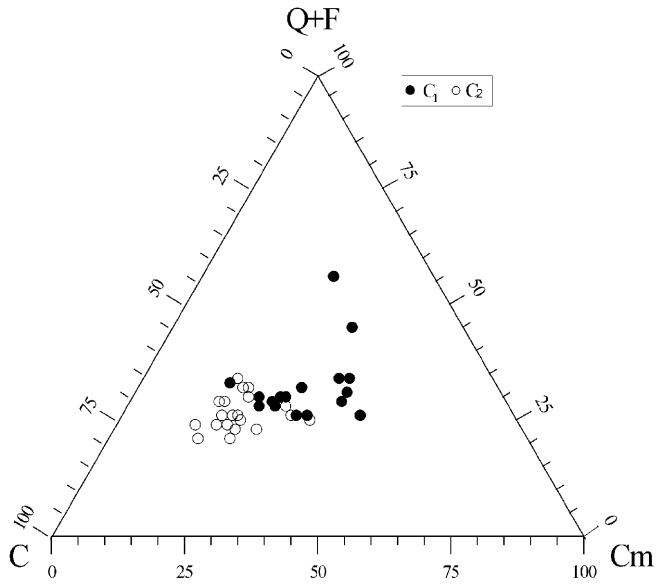

Fig. 16
Mineralogical composition of lithotype C

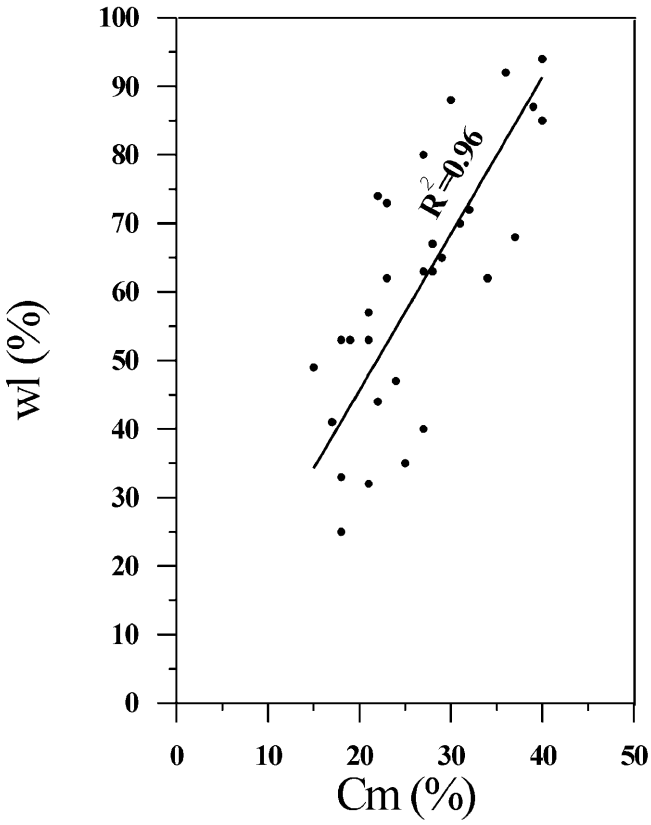

Fig. 17
Liquid limit (w_l) vs. clay mineral (Cm). The best fit line is reported ($R^2=0.96$)

calcite values. The clay minerals constitute on average 25% ($\sigma = 11\%$), quartz and feldspar 47% ($\sigma = 16\%$) and calcite 28% ($\sigma = 10\%$). The organic content is usually around 1.0%.

- Lithotype R: Due to the abundance of rock fragments the core obtained from this lithotype is scarce. Only six samples were collected and only two, from high-recovery intervals, were studied for their mineralogy and organic content. The material was classified as medium plasticity silty loam and clayey loam (Fig. 13a) with minor gravel (around 2%); this essentially represents the fine matrix in which the rock fragments are dispersed. The mineralogical composition of the matrix is not significantly different from that of the underlying lithotypes. The organic content is around 1%.
- Lithotype Dv: The physical characterisation of five samples indicated clay and silty clay of medium and high plasticity.

Geomechanical behaviour of Tiber alluvial system lithotypes

A series of physical tests was undertaken during the drilling of the boreholes shown in Fig. 9, including in-situ tests [standard penetration test (SPT); Lefranc permeability tests whose results were reported above], drill core tests (pocket penetrometer resistance and pocket vane tests) and laboratory tests on weakly disturbed samples (phase relationships tests; oedometer tests; uniaxial loading tests; direct shear tests and triaxial tests). The results of some of these tests, subdivided for lithotype, are given in Table 1.

The results of the other tests, which cannot be clearly tabulated, are qualitatively discussed below. In addition to the numerical data reported in the table, the following observations should be noted:

1. Two predominantly clayey-silt samples from lithotype D were found to be weakly overconsolidated. The moduli values obtained for lithotype D under uniaxial loading conditions were more elevated than those of the other groups.
2. The SPT tests indicate that lithotype C clays have a medium to stiff consistency, while the oedometer tests give overconsolidation ratio (OCR) values of 1.2. Below –14 m a.s.l. the material (lithotype C_2) has higher cohesion, unconfined compressive strength and deformability moduli values than the lithotype C_1 material above –14 m a.s.l.
3. The SPT tests indicate that the relative density (Dr) of lithotypes B_1 and B_2 averages between 50 and 60%.
4. The Nspt (number of blows required to advance the sampler 30 cm; Nspt = 26 to 13), pocket penetrometer resistance (250 to 100 kPa) and Ic (consistency index range) (Fig. 18) values of lithotype A all show a general decreasing trend with depth. Literature data (Bozzano et

Table 1
Range of the following geomechanical parameters. Number of tests carried out is in parentheses. w, Natural water content range; Ic, consistency index range; e_0, void ratio range; γ_n, total unit weight; Nspt, number of blows required to advance the sampler 30 cm; c′, cohesion intercept based on effective stress; ϕ', shear resistance angle based on effective stress; σ', confining pressure range in the direct shear tests; σ'_3, confining pressure range in the triaxial tests; q, unconfined compressive strength; Ei, initial tangent modulus; Es_1, secant modulus in stress range 0–0.5q

Lithotypes		Phase relationships				Standard penetration test Nspt (blows/30 cm)	Direct shear and triaxial tests			Uniaxial loading test		
		w (%)	Ic –	e_0 –	γ_n (kN/m^3)		c′ (kPa)	ϕ' °	σ'/σ'_3 (kPa)	q (kPa)	Ei (kPa)	Es_1 (kPa)
R		–	–	–		11–67 (19)			–			
A	A_1	48.6 (1)	0.3 (1)	1.3 (1)	18.4 (1)	12–24 (10)	–	–	–	–	–	–
	A_2	4.6–84.4 (15)	0.3–1.5 (15)	0.6–2.2 (15)	14.2–19.9 (15)	8–26 (26)	–	–	–	37–318 (5)	7000	5000
B	B_1	18.4–40.6 (12)	0.6–0.7 (12)	0.6–1.1 (12)	17–19.6 (12)	14–53 (13)	0–9.8 (4)	36–40 (4)	98–294	–	–	–
	B_2	19.4–39.5 (14)	0.6–1.5 (14)	0.5–1.0 (14)	16.4–20.6 (14)	4–27 (20)	0.9–12.8 (3)	31–35 (3)	98–294	13–153 (6)	7000	4000
C	Above –14 m a.s.l. C_1	22.2–70.3 (74)	0.3–1.5 (74)	0.6–1.9 (74)	14.5–19.7 (74)	6–24 (25)	16.6–49 (2)	15–20 (2)	147–441	14.4–174 (42)	5600	3500
	Below –14 m a.s.l. C_2	21.3–51.2 (36)	0.4–1.6 (36)	0.6–1.3 (36)	16.7–19.9 (36)	–	4.9–127.5 (4)	11–22 (4)	147–441	73.6–186 (22)	8800	8700
D		19.2–31.1 (26)	0.2–1.3 (26)	0.6–0.8 (26)	18.6–19.8 (26)	–	0–79.4 (3)	22–38 (3)	98–441	77.4–230 (3)	16000	15000
G		–	–	–		–	–	–	–	–	–	–

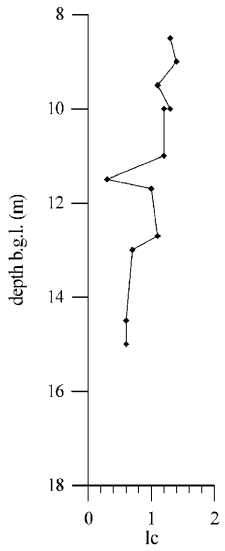

Fig. 18
Consistency index range (Ic) vs. depth b.g.l. for lithotype A samples

al. 1997) indicate that the OCR of 2.1 at 14 m b.g.l. also decreases with depth.

5. Penetrometer tests conducted on the anthropic fill material yielded highly variable values of between 10 and 40 blows/30 cm although >100 blows were recorded corresponding to local accumulations of rock fragments, pieces of walls and blocks of travertine used for construction. Bearing in mind the limited depth of the test, the penetrometer values indicate relative density values of around 40–60%.

The data obtained for lithotypes A, B and C can be extrapolated for the entire section shown in Fig. 9 as the physical–compositional characteristics are relatively homogeneous, either due to the sampling points being evenly distributed or because the number of analysed samples was high. In contrast, this extrapolation is not possible for lithotypes D and R and thus the data discussed are only significant at the point of sampling.

Theories regarding a geological–geotechnical model

The lithological, mineralogical and geotechnical data obtained for the deposits that fill the Tiber River valley along the section in Fig. 9 are supported by numerous other published information (Gigli 1971; Ventriglia 1971; Calabresi et al. 1980; Amanti et al. 1995; Bozzano et al. 1995, 1997; Chiodetti et al. 1996; Marinelli 1996) and unpublished work conducted in this part of the alluvial plain. As such, the knowledge acquired relative to the geological and morphological evolution of this area during the period 18,000 years b.p. to the present – and therefore to the interpretation of the section given in Fig. 9 – represents the foundation for the model given below which describes the filling of the buried Tiber River valley in the historical centre of Rome.

In the study area the fill sediments of the Tiber River valley consist of well-defined geometrical bodies whose lithologies can be distinguished. Each of these lithotypes exhibits a specific geomechanical behaviour which is partly defined by the parameters discussed above. The schematic diagram given in Fig. 19 outlines an alluvial system which has been divided into: (1) an historical layer (lithotypes R and A) and (2) a principal alluvial body (lithotypes B, C, D, G and Dv).

Historical layers deposited between the present and 3000–3500 years b.p.

This interval consists of anthropic fill material (lithotype R) overlying the grey-green silty sands and silty loams of lithotype A_1 and the hazel-coloured clay and clayey silts of lithotype A_2. The total thickness of the complex is between 8 and 22 m. Areas that have been settled for longer periods, or specific sites that underwent extensive construction for historical reasons, exhibit a greater thickness of the anthropic deposits (lithotype R). Between the Aureliane (275 a.d.) and Leonine walls (erected in 848 a.d. and enlarged during the sixteenth century), this unit has an average thickness of 7 to 8 m but can reach a maximum of some 25 m. In areas that were urbanised between the end of the last century and today, however, there is a minimum thickness of 3 to 5 m (see Figs. 2 and 11). Due to its origin, the macroscopic, compositional and geotechnical characteristics of this lithotype vary considerably. As a consequence, they cannot be extrapolated as regards either their description and/or laboratory data, away from the specific information points. Local aquifers exist in the anthropic fill material, bounded below by the less permeable lithotype A.

Lithotype A forms a continuous stratum below the anthropic fill material, although it is absent in some areas on the margin of the alluvial plain. The variations in thickness are in part compensated for by those in lithotype R. Lithotype A_1 occurs in a 700- to 800-m-wide belt adjacent to the present-day Tiber River and grades laterally to the more extensive lithotype A_2. A peculiar characteristic of this unit is its higher consistency, stiffness and shear strength relative to the underlying strata and with respect to its very recent depositional age. Such geomechanical behaviour corresponds to a state of weak overconsolidation, presumably due to desiccation in an area subject to oscillations in the water table (Lancellotta 1995).

Principal alluvial body (between 18,000 years and 3000–3500 b.p.)

The main part of this alluvial body comprises lithotype C, a 30- to 50 m thick grey clay and silty clay with a variable organic content. This unit is unique in that its macroscopic characteristics are quite homogeneous, although experimental data indicate a more subtle variation. Below a depth of 30 to 35 m from ground level (–14 m a.s.l.), for example, the material is relatively more stiff and resistant.

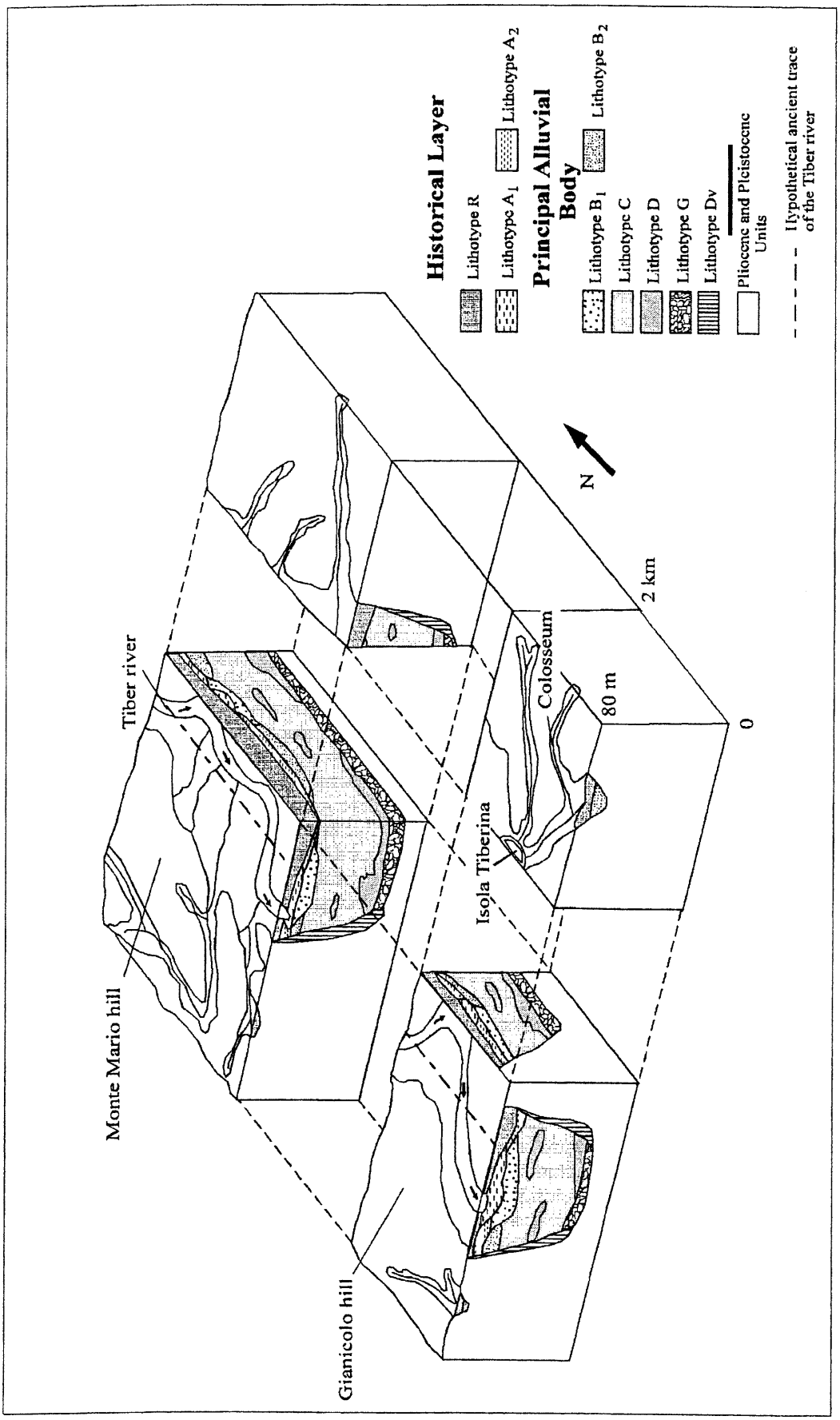

Fig. 19
Geological model sketch (not to scale)

In addition, organic-rich intercalations are found more frequently in the upper 30 to 35 m below ground level, including a particularly enriched level on the left bank at circa 32 m from the surface (some –13 m a.s.l.).
Lithotypes B_1 (medium-fine sands/sandy loam) and B_2 (alternating sandy loam and clay) overlie lithotype C along sharp contacts. The reconstruction of lithotype B_1 indicates that it occurs as a 1 km wide lenticular belt with a maximum thickness of some 15 m, centred about a hypothetical central trace of the present meandering Tiber River. Lithotype B_1 passes laterally to lithotype B_2, which is interpreted as material that filled the depressions caused by the more important Tiber River tributaries within the interior of the alluvial plain. The deposits ascribed to lithotypes B_1 and B_2 show a sharp variation in physical and geotechnical characteristics with respect to the materials that constitute lithotype C, within which they are embedded. Lithotypes B_1 and B_2 form aquifers which, near the Tiber River, can be subject to significant variations in the piezometric surface.
Within lithotype C, irregular bodies of alternating sandy-silty, silty-sandy, silty-clayey and clayey layers (lithotype D) can be observed. The present data on this irregular and heterogeneous unit do not permit its division into more homogeneous subunits, nor allow for an interpretation of its spatial distribution outside the studied section (Fig. 9). In any event, the presence of these intercalations within lithotype C implies significant lateral and vertical geomechanical variations and the possible occurrence of aquifers. Horizons ascribable to lithotype D can also be found between the basal gravel (lithotype G) and lithotype C.
Lithotype G, which varies in thickness between 2 and 10 m, is almost continuous at the base of the deposits that fill the Tiber valley in the urban area of Rome. This unit also forms a confined aquifer.

Conclusions

A geological–geotechnical model of the Tiber River valley is proposed. It is a global forecasting model (Fookes 1997) rather than a detailed one, which can be used as a starting point for projects that may be conducted in the Tiber River alluvial body and for defining a specific approach to technical problems linked to these projects. The limits of applicability of this model are imposed by the methodology used to build the model itself, but it can provide a basis on which to plan appropriate geotechnical testing in order to define the local situation with the required detail. The opportunity for upgrading the proposed model lies in the continued addition of progressively acquired and elaborated new data.

Acknowledgements The authors would like to thank Dr. L. Manfra and Prof. S. Improta (University of Rome "La Sapienza"") for the absolute dating of three samples, Prof. G. Valentini (University of Rome "La Sapienza) for his very valuable suggestions and Dott. F. Marra and Dr. C. Rosa for their helpful discussions. The research was supported financially by a CNR grant (CTB 96.00360.05).

References

Alessio M, Allegri L, Antonioli F, Belluomini G, Ferranti L, Improta S, Manfra L, Proposito A (1992) Risultati preliminari relativi alla datazione di speleotemi sommersi nelle fasce costiere del Tirreno Centrale (Italy). G Geol 54(2):165–193

Amanti M, Gisotti G, Pecci M (1995) I dissesti di Roma. In: Funiciello R (ed) La geologia di Roma. Il Centro Storico. Mem Desc Carta Geol Ital 50:219–248

Ambrosetti P, Bonadonna FP (1967) Revisione dei dati del Plio-Pleistocene di Roma. Atti Acc G Sci Nat Catania 18:33–70

Ambrosini S, Castenetto S, Cevolani F, Di Loreto E, Funiciello R, Liperi L, Molin D (1986) Risposta sismica dell'area urbana di Roma in occasione del terremoto del Fucino del 13 gennaio 1915. Mem Soc Geol Ital 35:445–452

American Society for Testing and Materials (1988) Annual book of ASTM standards. Soil and rock, building stones, geotextiles, vol 04.08. D 422-63:Standard method for particle-size analysis of soils. D 4318-84:Standard test method for liquid limit, plastic limit and plasticity, index of soils. ASTM, Philadelphia

Bellotti P, Chiocchini U, Castorina F, Tolomeo L (1994) Le unità clastiche plio-pleistoceniche tra Monte Mario (città di Roma) e la costa tirrenica presso Focene: alcune osservazioni sulla stratigrafia sequenziale. Boll Serv Geol Ital CXIII:3–24

Bellotti P, Milli S, Tortora P, Valeri P (1995) Physical stratigraphy and sedimentology of the Late Pleistocene-Holocene Tiber Delta depositional sequence. Sedimentology 42:617–634

Bellotti P, Caputo C, Ciccacci S, De Rita D, Donati S, Fredi P, Funiciello R, La Monica GB, Landini B, Marra F, Milli S, Parotto M, Pugliese F (1997) Fundaments for a geomorphological overview on Rome and its surroundings. Suppl Geogr Fis Dinam Q III(T.2):105–121

Belluomini G, Iuzzolini P, Manfra L, Mortari R, Zalaffi M (1986) Evoluzione recente del delta del Tevere. Geol Rom 25:213–234

Bencivenga M, Di Loreto E, Liperi L (1995) Il regime idrologico del Tevere, con particolare riguardo alle piene nella città di Roma. In: Funiciello R (ed) La geologia di Roma. Il Centro Storico. Mem Desc Carta Geol Ital 50:125–168

Boschi E, Caserta A, Conti C, Di Bona M, Funiciello R, Malagnini L, Marra F, Martines G, Rovelli A, Salvi S (1995) Resonance of subsurfaces sediments: an unforeseen complication for designers of Roman columns. Bull Seismol Soc Am 85 1:320–324

Bozzano F, Funiciello R, Marra F, Rovelli A, Valentini G (1995) Il sottosuolo dell'area dell'Anfiteatro Flavio in Roma. Geol Appl Idrogeol 30:405–422

Bozzano F, Funiciello R, Gaeta M, Marra F, Rosa C, Valentini G (1997) Recent alluvial deposits in Rome (Italy): morpho-stratigraphic, mineralogical and geomechanical characterisation. Proc Int Symp Engineering Geology and the Environment, Publ 1, pp 1193–1198

Bozzano F, Gaeta M, Terrinoni M (1998) Slope stability of Monte Mario urban park in Rome (Italy). Proc 8th IAEG Congr, Vancouver, Publ 3, pp 1601–1608

Broadbent FE (1965) Organic matter. Methods of soil analysis; agronomy, chap 9. American Society of Agronomy; Madison, Wisconsin, 92 pp

Calabresi G, Cassinis C, Nisio P (1980) Influenza del regime del Tevere sul comportamento di un fabbricato monumentale adiacente. Proc 14th Convegno Nazionale di Geotecnica AGI, Firenze, Publ 1, pp 25–33

Carboni MG, Iorio D (1997) Nuovi dati sul Plio-Pleistocene marino del sottosuolo di Roma. Boll Soc Geol Ital 116:435–451

Casagrande A (1948) Classification and identification of soils. Trans Am Soc Civ Eng 113:901

Chappel J, Shackleton NJ (1986) Oxygen isotopes and sea level. Nature 324:137–140

Chiodetti G, Di Pasquale G, Feliziani A, Merlo S, Milana G, Orsini G, Pascarella F, Pino G, Pugliese A, Serva L, Trojano R, Zechini A (1996) Analisi delle problematiche relative alle metodologie geologiche, geotecniche ed ingegneristiche utilizzate per la realizzazione delle gallerie di linea e di stazione dei nuovi tratti della metropolitana di Roma e confronto con metodi alternativi. In: Serva L (ed) Progetto strategico gallerie. Agenzia Nazionale Protezione Ambiente, Consiglio Nazionale delle Ricerche, Roma, pp 7–59

Cifelli F, Donati S, Funiciello F, Gasparini C, Saraceni A, Tertulliani A (1997) Il risentimento a Roma del terremoto Umbro-Marchigiano del 14 ottobre 1997. Pubbl Ist Naz Geofis 593:45–49

Cipriani GB (1830) Roma di G.B. Cipriani. In: Frutaz AP (1962) Le piante di Roma. Pianta CXCII, Tav. 498. Istituto di Studi Romani, Roma

Contini F (1661) Strada fuori di Porta Angelica e Porta Castello-Catasto Alessandrino. In: Frutaz AP (1972) Le carte del Lazio II. Pianta XXIX 20a, Tav. 137. Istituto di Studi Romani, Roma

Corazza A, Lombardi L (1995) Idrogeologia del centro Storico di Roma. In: Funiciello R (ed) La geologia di Roma. Il Centro Storico. Mem Desc Carta Geol Ital 50:179–208

Crescenzi R, Piro M, Vallesi R (1995) Le cavità sotterranee a Roma. In: Funiciello R (ed) La geologia di Roma. Il Centro Storico. Mem Desc Carta Geol Ital 50:249–283

Donati S, Funiciello R, Rovelli A (1999) Seismic response in archaeological areas: the case-histories of Rome. J Appl Geophys 41:229–239

Faccenna C, Funiciello R, Marra F (1995) Inquadramento geologico strutturale dell'area romana. In: Funiciello R (ed) La geologia di Roma. Il Centro Storico. Mem Desc Carta Geol Ital 50:31–47

Fah D, iodice C, Suhadolc P, Panza GF (1993) A new method for the realistic estimation of seismic ground motion in megacities: the case of Rome. Earthquake Spectra 9:643–668

Federici V, Santoro VM (1997) Antiche cavità sotterranee sul Colle Aventino (Roma): indagini, studi e rilievi eseguiti nella zona di Via San Giosafat e valutazione delle caratteristiche di potenzialità di dissesto. Geol Tec Ambient 3(97):63–78

Fookes PG (1997) Geology for engineers: the geological model, prediction and performance. Q J Eng Geol 30:293–424

Fossa Mancini E (1922) Il nuovo quartiere di Roma (Monteverde) e le frane. G Geol Pratica 3:54–66

Funiciello R (ed) (1995) La Geologia di Roma. Il Centro storico. Mem Desc Carta Geol Ital 50:550

Gigli E (1971) La pianura del Tevere. Capitolium XLVI(5,6):46–72

Insolera I (1980) Roma immagini e realtà dal X al XX secolo. In: De Seta C (ed) Le città nella storia d'Italia. Laterza, Roma, 468 pp

Karner DB, Marra F (1998) Correlation of fluviodeltaic aggradational sections with glacial climate history: a revision of the Pleistocene stratigraphy of Rome. Geol Soc Am Bull 10(6):748–758

Lancellotta R (1995) Geotechnical engineering. Technical University of Turin, Italy, 448 pp

Lanzini M (1995) Il problema delle cavità sotterranee a Roma-un rischio geologico. Geol Ambient II(3):2–8

Lugli L (1961) Il tratto urbano della via Flaminia. Via del Corso 10:21–30

Marinelli S (1996) Depositi alluvionali recenti nell'area della città di Roma: distribuzione spaziale e caratterizzazione geomeccanica. Tesi di Laurea, Università degli Studi di Roma La Sapienza, Dipartimento di Scienze della Terra, Roma

Marra F (1993) Stratigrafia ed assetto geologico-strutturale dell'area romana compresa tra il Tevere e Rio Galeria. Geol Rom 29:515–535

Marra F, Rosa C (1995a) Stratigrafia ed assetto geologico dell'area romana. In: Funiciello R (ed) La geologia di Roma. Il Centro Storico. Mem Desc Carta Geol Ital 50:49–112

Marra F, Rosa C (1995b) Carta geologica del Centro Storico di Roma in scala 1:10.000. In: Funiciello R (ed) La geologia di Roma. Il Centro Storico. Tav. 9. Mem Desc Carta Geol Ital 50

Marra F, Florindo F, Karner DB (1998) Paleomagnetism and geochronology of early Middle Pleistocene depositional sequences near Rome: comparison with the deep-sea δ^{18} O record. Earth Planet Sci Lett 159:147–164

Miall AD (1996) The geology of fluvial deposits: sedimentary facies, basin analysis, and petroleum geology. Springer, Berlin Heidelberg New York, 582 pp

Milli S (1997) Depositional setting and high-frequency sequence stratigraphy of the middle-upper Pleistocene to Holocene deposits of the Roman basin. Geol Rom 33:99–136

Moczo P, Rovelli A, Labak P, Malagnini L (1995) Seismic response of the geologic structure underlying the Roman Colosseum and a 2-D resonance of a sediment valley. Ann Geofis V. · VIII(5–6):939–955

Oberholtzer F (1875) Le foci del Tevere. GB Paravia, Roma, 93 pp

Pinna M (1977) Climatologia. UTET, Torino, 442 pp

Ravaglioli A (1998) Il Tevere fiume di Roma. Storia, curiosità, prospettive. Tascabili Economici Newton, Roma, Publ 30, 66 pp

Rosa AC (1924) Practical field tests for subgrade soils. Public Roads 5(6):10–15

Sagnotti L, Mattei M, Faccenna C, Funiciello R (1994) Paleomagnetic evidence for no tectonic rotation of the central Italy Tyrrhenian margin since Upper Pliocene. Geophys Res Lett 21:481–484

Staderini M (1998) Roma repubblicana e imperiale. Edizioni Abete, Roma, 159 pp

Stuiver M, Reimer PJ (1993) Extended ^{14}C data base revised Calib. 3.0 ^{14}C Age Calibration Program. Radiocarbon 35(1):215–230

Tellini A (1893) Carta Geologica dei dintorni di Roma. Regione alla destra del Tevere. In: Funiciello R (ed) La geologia di Roma. Il Centro Storico, Tav. 6. Mem Desc Carta Geol Ital

Ufficiali di Stato Maggiore Francese (1868) Pianta di Roma e dintorni. In: Frutaz AP (1962) Le piante di Roma III. Pianta CCVIII, Tav. 532. Istituto di Studi Romani, Roma

Ventriglia U (1971) La geologia della città di Roma. Amministrazione Provinciale di Roma, Roma, 417 pp

Voltaggio M, Andretta D, Taddeucci A (1994) ^{230}Th-^{238}U data in conflict with ^{40}Ar ^{39}Ar leucite ages for Quaternary volcanic rocks of the Alban Hills, Italy. Eur J Mineral 6:209–216

Weimer RJ (1986) Relationship of unconformities, tectonics, and sea level change in the Cretaceous of the Western Interior, United States. In: Peterson JA (ed) Paleotectonics and sedimentation in the Rocky Mountain region, United States. Am Assoc Petrol Geol Mem 41:397–422